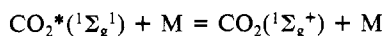
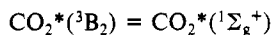
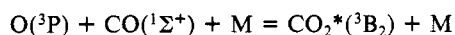
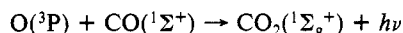


As shown in Figure 5, our present plot is rather similar to that of Baulch et al.¹⁵

Lin and Bauer⁶ obtained $k_6 = 2.8 \times 10^{12} \exp(99.6 \text{ kJ}) \text{ cm}^6 \text{ mol}^{-2} \text{ s}^{-1}$. In order to explain the negative activation energy, they proposed the following mechanism for the reaction:



Here, $\text{CO}_2(^3\text{B}_2)$ and $\text{CO}_2(^1\Sigma_g^+)$ represent vibrationally excited CO_2 in the $^3\text{B}_2$ and $^1\Sigma_g^+$ states, respectively. Further, they assumed that the rate-determining step is a transition between the $^3\text{B}_2$ state and the $^1\Sigma_g^+$ state and calculated that the crossing point between the $^3\text{B}_2$ and $^1\Sigma_g^+$ states is 31.4 kJ/mol below the $^3\text{B}_2$ dissociation limit. On the other hand, Clyne and Thrush¹⁹ studied the reaction



(18) Warnatz, J. In *Combustion Chemistry*, Gardiner, Jr., W. C., Ed.; Springer-Verlag: New York, 1984; p 197.

and found that the reaction is third order with a positive activation energy of 15.5 kJ. They claimed that the rate of CO_2 formation is not limited by spin change but by an energy barrier in the $^3\text{B}_2$ CO_2 potential curve which correlates with $\text{O}(^3\text{P}) + \text{CO}(^1\Sigma^1)$. They concluded that crossing from the $^3\text{B}_2$ state to the $^1\text{B}_2$, from which emission occurs, is rapid compared to the rate of barrier crossing. Later, Slanger et al.²⁰ obtained $k_6 = 2.3 \times 10^{15} \exp(-18.2 \text{ kJ}/RT) \text{ cm}^6 \text{ mol}^{-2} \text{ s}^{-1}$ over the temperature range 250–370 K, which was recommended by Baulch et al.¹⁵ They supported the above-described claim of Clyne and Thrush and calculated that there is a different mechanism taking place at the higher temperatures used in Lin and Bauer than that at the lower temperatures, if the shock tube experiment does not suffer from impurity problems.

The value of k_6 obtained by us supports the conclusions of Clyne and Thrush and Slanger et al. and indicates that reaction 6 proceeds via the same mechanism at both higher and lower temperatures.

(19) Clyne, M. A. A.; Thrush, B. A. *Proc. R. Soc. (London) Ser. A* **1962**, *A269*, 404.

(20) Slanger, T. G.; Wood, B. J.; Black, G. J. *Chem. Phys.* **1972**, *57*, 233.

High-Temperature Pyrolysis of Toluene

K. M. Pamidimukkala, R. D. Kern,

Department of Chemistry, University of New Orleans, New Orleans, Louisiana 70148

M. R. Patel, H. C. Wei, and J. H. Kiefer*

Department of Chemical Engineering, University of Illinois at Chicago, Chicago, Illinois 60680

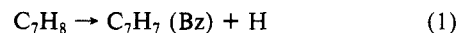
(Received: August 5, 1986; In Final Form: November 10, 1986)

The thermal decomposition of toluene has been investigated by two independent shock tube techniques: time-of-flight (TOF) mass spectrometry and laser-schlieren densitometry. These studies cover the temperature range 1550–2200 K for pressures 0.2–0.5 atm. C_2H_2 , C_4H_2 , CH_4 , and C_7H_7 were identified as major species along with lesser amounts of C_2H_4 , C_6H_2 , and C_6H_6 . The laser-schlieren profiles require a dominance by CC scission to phenyl and methyl with a rate constant $\log k \text{ (s}^{-1}\text{)} = 12.95 - 72.6 \text{ (kcal)}/2.3RT$ for 1600–2100 K and 0.5 atm. Such dominance is also required to produce the methane seen in the TOF spectra. A mechanism is proposed which provides an excellent description of density gradient and major species concentration profiles over this range.

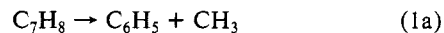
Introduction

Nearly all of the complications encountered in unimolecular decay kinetics occur in the decomposition of toluene: (a) the possibility of more than one dissociation channel, (b) an important contribution by recombination and other secondary processes, (c) falloff effects in both primary and secondary unimolecular processes, (d) discrepancies in the measured rate constants for key reactions, and (e) some uncertainty in the thermodynamic properties of important species.

Despite the above problems, toluene pyrolysis has generated much interest, undoubtedly motivated by toluene's popularity as a radical scavenger.¹ Here we are concerned with the pyrolysis kinetics at high temperatures ($T > 1000 \text{ }^\circ\text{C}$), and the very extensive lower temperature literature will not be generally considered (see Smith^{2,3} for a listing). We are particularly interested in the possible contribution of C–C bond scission to the dissociation. Following Szwarc's original work,⁴ this dissociation is usually taken to be confined to



(Bz denotes benzyl radical), but many workers (see Smith^{2,3}) have suggested the C–C scission



also runs in parallel.

There is no doubt that (1a) must occur; the issue is merely to what extent and under what conditions. Since the bond dissociation energies (BDE's) for (1) and (1a) differ by 15 kcal/mol (see below), the prejudice favoring reaction 1 is understandable. However, it is a common observation that separation into large radicals is accompanied by large A factors, exceeding 10^{17} s^{-1} in some instances, whereas that of (1) is probably little more than 10^{15} s^{-1} .⁵ On this rough basis, one might expect near equality of the high-pressure rates when the temperature reaches 1600 K.

The toluene pyrolysis is of course a chain reaction, as has been known and undisputed since the early work of Szwarc.⁴ Nevertheless, at high temperatures the product distribution can be

(1) Szwarc, M. *Chem. Rev.* **1950**, *47*, 75.

(2) Smith, R. D. *Combust. Flame* **1979**, *35*, 179.

(3) Smith, R. D. *J. Phys. Chem.* **1979**, *83*, 1553.

(4) Szwarc, M. *J. Chem. Phys.* **1948**, *16*, 128.

(5) Benson, S. W.; O'Neal, H. E. "Kinetic Data on Gas Phase Unimolecular Reactions"; *Natl. Stand. Ref. Data Ser. (U.S., Natl. Bur. Stand.)* **1970**, No. 21.

dominated by simple dissociation, and Colket and Seery,⁶ from a recent single-pulse shock tube study covering 1100–2700 K, have suggested that (1a) always controls this distribution. Their suggestion is not that (1a) is faster than (1) over this range—they actually employed a rate constant for (1) much larger than (1a) in their model—but rather since benzyl is stable and the equilibrium constant for (1) is small, reaction 1 equilibrates very quickly, before significant dissociation can occur. Whereas, since (1a) generates the unstable phenyl radical,^{7,8} it is effectively irreversible and thus governs the progress and products of the decomposition. They obtain a rate constant $\log k_{1a} \text{ (s}^{-1}\text{)} = 12.2\text{--}70 \text{ (kcal)}/2.3RT$ for the C–C scission.

A number of other high-temperature investigations of toluene pyrolysis need mention. Smith^{2,3} has observed the products with Knudsen cell mass spectrometry over 1173–2073 K. Around 1600 K major products were C₂H₂, C₂H₃, C₂H₄, CH₄, C₄H₂, and C₆H₆. Smith interpreted his results as evidence for dissociation via (1) only.

Recent shock tube studies of toluene decomposition include mid-UV absorption measurements of both toluene⁹ and benzyl radical¹⁰ dissociation and an ARAS investigation of H atom formation rates.¹¹ Although these experiments were again interpreted with dissociation through (1) only, and all used highly dilute mixtures of toluene in argon, their derived rate constants for (1) differ by at least a factor of 6 at 1600 K. A possible reason for misinterpretation of the mid-UV absorption studies has been suggested.¹² This matter will also be considered here.

In this paper we present the results of two time-resolved shock tube investigations of toluene pyrolysis at high temperatures. From laser-schlieren (LS) measurements of density gradient and time-of-flight (TOF) mass spectral product profiles, we present additional evidence for a dominance of C–C scission in high-temperature toluene dissociation, as well as an independent measure of the rate of this reaction.

Experimental Section

The apparatus and procedures for both techniques have been fully described.¹³ For the TOF work, toluene (Baker analyzed reagent grade) was purified by repeated bulb-to-bulb distillations, finally taking the middle fraction to a 5-L sample bulb. Each mixture was diluted with Matheson research grade neon (99.999%) to the desired concentration.

The TOF data reduction process entailed the separation of cracking pattern contributions from the mass peak signals of interest. An ionization energy of 32 eV was employed. The cracking pattern of toluene, under our experimental conditions, was obtained by shocking toluene mixtures at conditions where little reaction occurs (1100–1200 K) and also by recording the cracking spectrum at room temperature. The major cracking component was C₇H₇ (C₇H₇/C₇H₈ ~ 0.98) followed by C₅ and C₄ species. In reacting mixtures, it was not clear whether *m/e* species lower than C₇ were the cracking products of benzyl radical or parent molecule. Examination of the cracking pattern of a 1.8% C₇H₇/Cl mixture at room temperature and at nonreacting conditions (1100 K) revealed that species with *m/e* less than 91 appear to be secondary cracking products of C₇H₇, not C₇H₈. The major cracking products were C₃H₅, C₃H₃, C₄H₄, and C₄H₂ with lesser amounts of C₆H₅. Before concentration plots were constructed, respective amounts of cracking contributions were subtracted from their corresponding signals. Additional runs were performed with

C₇D₈ in order to increase the mass resolution between benzyl and toluene. The various temporal peak heights were each divided by the respective inert gas peaks. Conversion of the resulting peak height ratios to concentration profiles was achieved by the use of calibration plots. The calibration runs were performed at essentially nonreacting, constant-density conditions.

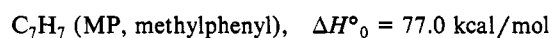
For the laser-schlieren (LS) experiments, toluene (Aldrich) was degassed and vacuum distilled to a 50-L glass vessel where it was mixed with krypton (Spectra-Gases UHP) to form mixtures of 0.5%, 1%, 2%, and 4% toluene. GC analysis of the original liquid showed trace impurities below the 0.7% level. Density gradients were calculated from measured beam deflections assuming constant refractivities for toluene and krypton.¹⁴ A total of 82 experiments were analyzed covering postshock frozen temperatures from 1400 to 2300 K and pressures of 100–1000 Torr.

Since toluene pyrolysis is well-known to generate particulates (soot), the possibility of attenuation of the 6328 Å laser radiation must be recognized. To test this, total intensity measurements were made in a few experiments. As in benzene decomposition,⁸ some attenuation was observed, but only long after completion of the density gradient measurements.

Calculations

Modeling of TOF product profiles used the CHEMKIN¹⁵ routine. The integration program used in the LS analysis has also been described.¹⁶

Thermodynamic functions were mainly taken from the usual sources.¹⁷ For some of the more critical species, the assumed heats of formation were



The last is a generic methylphenyl, with all three possible isomers assigned the same properties (and reaction rates). This heat of formation simply assumes the same BDE for ring hydrogens of toluene and benzene. The C₄H₃ radical generated by phenyl dissociation⁸ was again taken to be the less stable isomer, CH=CH–C≡CH, with $\Delta H^\circ_0 \sim 128 \text{ kcal/mol}$. As in the benzene pyrolysis,⁸ the properties of this radical are not significant parameters.

The equilibrium constant for reaction 1 used here is⁹

$$\log K_1 \text{ (mol/cm}^3\text{)} = 1.931 - 89.3 \text{ (kcal)}/2.3RT$$

In a previous analysis of ethylbenzene decomposition, the properties of benzyl radical used in this calculation of K_1 were questioned.⁹ It was suggested that this K_1 may be too high by about a factor of 2. Nonetheless, the unaltered properties given in ref 9 were used herein.

The enthalpies of the species C₂H, C₄H, and C₆H₂, involved in acetylene decomposition, were those of ref 27. Any changes in these properties would of course require a corresponding alteration of the kinetic parameters, also taken from ref 27. Re-

(14) Gardiner, W. C., Jr.; Hidaka, Y.; Tanzawa, T. *Combust. Flame* **1981**, *40*, 213.

(15) (a) Kee, R. J.; Miller, J. A.; Jefferson, T. H. "CHEMKIN: A General Purpose, Problem Independent Transportable, Fortran Chemical Kinetics Code Package", Sandia National Laboratories, 1980, SAND 80-8003. (b) Hindmarsh, A. C. "LSODE and LSODI, Two New Initial Value Differential Equation Solvers", ACM SIGNUM Newsletter, 1980, 15, No. 4.

(16) Gardiner, W. C., Jr.; Walker, B. F.; Wakefield, C. B. In *Shock Waves in Chemistry*; Lifshitz, A., Ed.; Marcel Dekker: New York, 1981; p 319.

(17) "Selected Values of Properties of Hydrocarbons and Related Compounds", American Petroleum Institute Research Project 44, 1975. "JANAF Thermochemical Tables", *Natl. Stand. Ref. Data Ser. (U.S., Natl. Bur. Stand.)* 1971, No. 37.

(18) Kern, R. D.; Singh, H. J.; Esslinger, M. A.; Winkler, P. W. *Symp. (Int.) Combust., [Proc.]*, 19th 1982, 1351.

(6) Colket, M. B.; Seery, D. J. Presented at 20th Symposium (International) on Combustion, Ann Arbor, MI, 1984.

(7) Rao, V. S.; Skinner, G. B. *J. Phys. Chem.* **1984**, *88*, 5990.

(8) Kiefer, J. H.; Mizerka, L. J.; Patel, M. R.; Wei, H.-C. *J. Phys. Chem.* **1985**, *89*, 2013.

(9) Astholz, D. C.; Durant, J.; Troe, J. *Symp. (Int.) Combust., [Proc.]*, 18th 1981, 885.

(10) Astholz, D. C.; Troe, J. *J. Chem. Soc., Faraday Trans. 2* **1982**, *78*, 1413.

(11) Rao, V. S.; Skinner, G. B. *J. Phys. Chem.* **1984**, *88*, 4362.

(12) Mizerka, L. J.; Kiefer, J. H. *Int. J. Chem. Kinet.* **1986**, *18*, 363.

(13) Kern, R. D.; Wu, C. H.; Skinner, G. B.; Rao, V. S.; Kiefer, J. H.; Towers, J. A.; Mizerka, L. *J. Symp. (Int.) Combust., [Proc.]*, 20th 1984, 789.

TABLE I: Kinetic Mechanism for Toluene Pyrolysis

reaction no.	reaction ^a	log A, ^b cgs	n	E _a , kcal/mol	source
1	C ₇ H ₈ → C ₇ H ₇ (Bz) + H	<i>d</i>	<i>d</i>	<i>d</i>	present work
1a	C ₇ H ₈ → C ₆ H ₅ + CH ₃	12.95	0	72.6	present work
2	C ₇ H ₈ + H → C ₇ H ₇ (Bz) + H ₂	-4.12	5.5	0.34	11
3	C ₇ H ₈ + H → C ₇ H ₇ (MP) + H ₂	14.40	0	16.0	see text
4	C ₇ H ₈ + CH ₃ → C ₇ H ₇ (Bz) + CH ₄	-3.36	5.0	8.3	12
5	C ₇ H ₈ + CH ₃ → C ₇ H ₇ (MP) + CH ₄	-3.36	5.0	12.3	estimate
6	C ₇ H ₇ (MP) → C ₄ H ₃ + C ₃ H ₄	16.00	0	82.0	estimate ^c
7	C ₇ H ₇ (MP) → C ₃ H ₃ + 2C ₂ H ₂	16.00	0	83.0	estimate ^c
8	C ₇ H ₇ (Bz) → C ₃ H ₃ + 2C ₂ H ₂	14.25	0	84.8	10, 12
9	CH ₃ + C ₆ H ₆ → CH ₄ + C ₆ H ₅	-3.36	5.0	12.3	estimate
10	C ₃ H ₄ + M → C ₃ H ₃ + H + M	17.30	0	65.0	estimate
11	C ₃ H ₄ + H → C ₃ H ₃ + H ₂	14.84	0	14.5	estimate
12	C ₆ H ₆ → C ₆ H ₅ + H	<i>e</i>	<i>e</i>	<i>e</i>	
13	C ₆ H ₆ + H → C ₆ H ₅ + H ₂	14.40	0	16.0	8
14	C ₆ H ₅ + M → C ₄ H ₃ + C ₂ H ₂ + M	15.70	0	37.0	8
15	C ₄ H ₃ + M → C ₄ H ₂ + H + M	51.68	-10.0	63.0	8
16	C ₂ H ₆ + H → C ₂ H ₄ + H + H ₂	14.60	0	15.0	28
17	H ₂ + M → 2H + M	12.35	0.5	92.5	27
18	C ₂ H ₂ + M → C ₂ H + H + M	16.62	0	107.0	27
19	C ₂ H + H ₂ → C ₂ H ₂ + H	12.87	0	0	27
20	C ₂ H + C ₂ H ₂ → C ₄ H ₂ + H	13.60	0	0	27
21	C ₄ H ₂ → C ₄ H + H	14.89	0	120.0	27
22	C ₂ H + C ₄ H ₂ → C ₆ H ₂ + H	13.60	0	0	27
23	C ₄ H + C ₂ H ₂ → C ₆ H ₂ + H	13.60	0	0	27
24	C ₄ H + H ₂ → H + C ₄ H ₂	13.30	0	0	27
25	C ₂ H ₆ + CH ₃ → C ₂ H ₄ + H + CH ₄	-3.36	5.0	8.3	28
26	M + C ₂ H ₆ → M + 2CH ₃	<i>f</i>	<i>f</i>	<i>f</i>	

^aThe reverse of each reaction is included through detailed balance. ^bThe rate constants have the form $AT^n \exp(-E_a/RT)$. ^cBoth reactions represent a two-step process and are sufficiently rapid for the properties of the C₇H₇ (MP) to be irrelevant. ^d $k_{1a}/k_1 \sim 2-4$ depending on temperature. ^ePressure dependent; see ref 8. ^fPressure dependent; see ref 12.

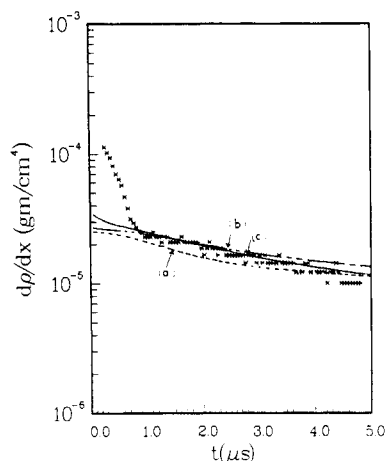


Figure 1. Density gradient profile for a shock in 2% toluene-krypton, with frozen initial conditions $T = 1680$ K, $P = 656$ Torr. The experimental gradients are (X), and the lines represent the results of calculations using various mechanisms. Here (a) allows dissociation only through reaction 1; this is effectively the classic Szwarz mechanism as specified by Rao and Skinner.¹¹ (b) is the mechanism of Table I without reaction 1, and (c) is the full mechanism of Table I.

actions of these species were merely included to ensure completeness; they actually make no significant contribution to this pyrolysis for any present conditions.

The RRKM program used here was the direct vibrational state count with classical rotation routine described previously.⁸

Results and Discussion

Representative LS density gradient profiles are presented in Figures 1-3. Also shown in these figures are the results of calculations using the mechanism of Table I. The majority of these semilog profiles show a quite consistent linearity, and it is then a simple matter to extrapolate to an unambiguous initial endothermic rate. The results of such extrapolation are shown in Figure 4. These tentative first-order "rate constants" (k_1) are based on a heat of reaction $\Delta H^\circ_{298} = 88$ kcal/mol, in effect assuming dissociation through reaction 1 only. If both channels

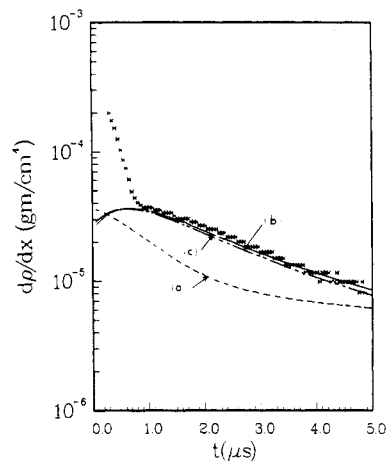


Figure 2. Density gradient profile for 0.5% C₇H₈-Kr with initial $T = 1942$ K, $P = 241$ Torr. The data and calculations are identified as in Figure 1.

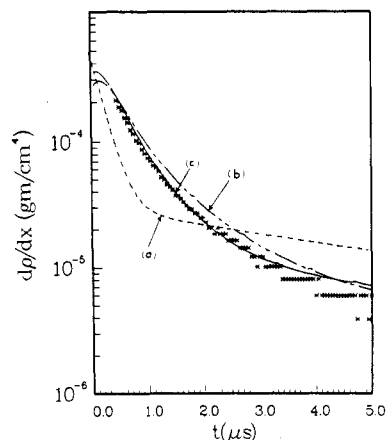


Figure 3. Density gradient profile for 1% C₇H₈-Kr with initial $T = 2135$ K, $P = 371$ Torr. The data and calculations are identified as in Figure 1.

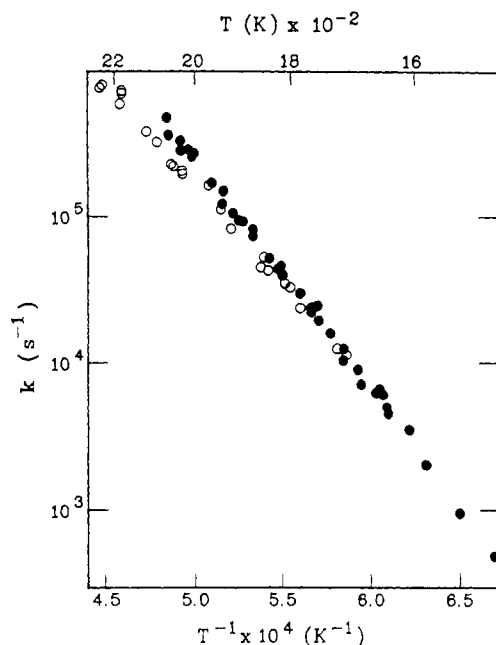


Figure 4. Initial endothermic "rate constants" obtained from the laser-schlieren density gradient profiles by extrapolation to $t = 0$. Here, ● represents frozen pressures around 400 Torr and ○ around 200 Torr. A heat of reaction of 88 kcal/mol was used to convert the zero-time gradients to rate constants. Note that the drop in rate from 400 to 200 Torr at 2000 K is 40–50%. The slope of the quite linear 400-Torr data corresponds to an E_a of 72.6 kcal/mol.

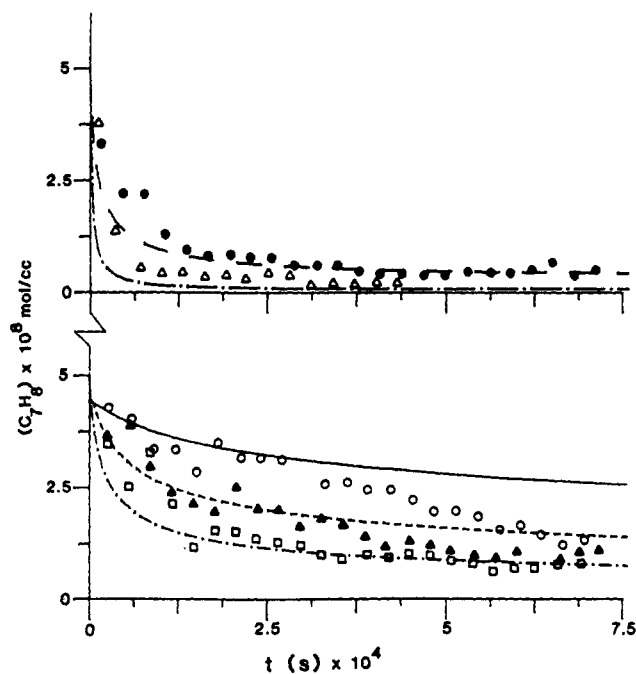
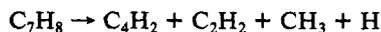


Figure 5. Toluene profiles utilizing TOF data from 1.8% C_7H_8 -Ne mixture; initial toluene concentration range was $(4.36-4.92) \times 10^{-8}$ mol/cm³: ○, 1590 K; ▲, 1722 K; □, 1832 K; ●, 1925 K; △, 2145 K. The lines represent model calculations using the mechanism given in Table I.

1 and 1a are involved, then (roughly) $k_t \sim k_1 + 2.6k_{1a}$. The factor 2.6 arises from the much greater effective heat of reaction for (1a), which is here presumed to be quickly followed by phenyl dissociation, i.e., the highly endothermic reactions 14 and 15 of Table I,^{7,8} making the net reaction from (1a)



with a $\Delta H^\circ_{298} \approx 242$ kcal/mol. At 298 K the ratio of effective heats for (1a) and (1) is then 2.75, but over 1600–2200 K this ratio drops to an average of about 2.6.

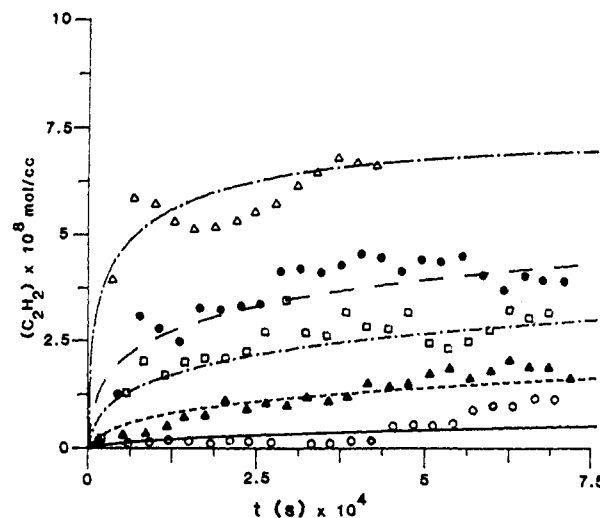


Figure 6. Acetylene growth profiles. Symbols refer to same temperatures as in Figure 5.

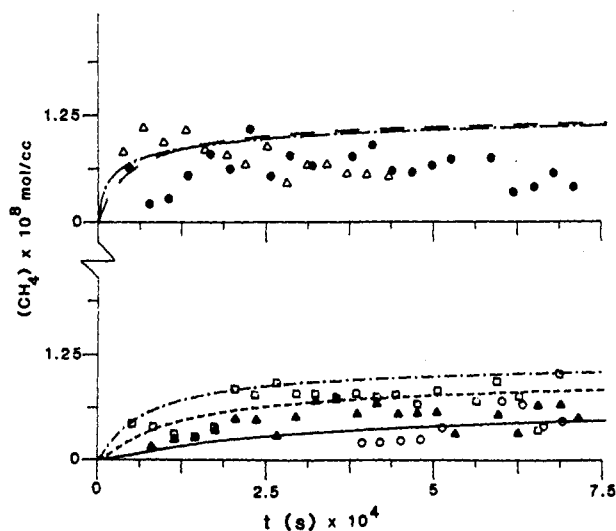


Figure 7. CH_4 growth profiles. Symbols refer to same temperatures as in Figure 5.

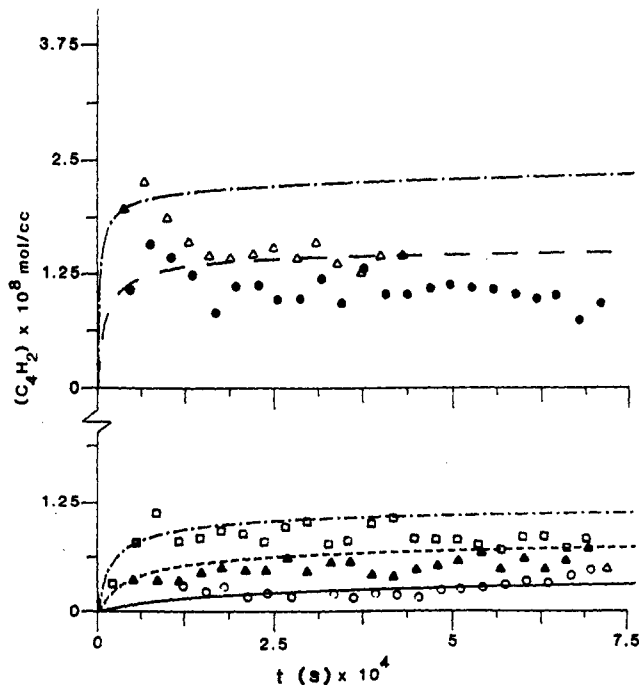
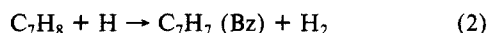


Figure 8. C_4H_2 growth profiles. Symbols refer to same temperatures as in Figure 5.

TOF concentration profiles of major species, normalized to constant density, are shown in Figures 5–8. The model profiles were normalized to constant inert gas concentration in order to conform with the calibration procedure, also at constant density, as described in the Experimental Section. The concentration profiles were constructed from a series of experiments in 1.8% toluene–neon for the frozen temperature range 1590–2145 K and total pressures of 0.3–0.5 atm. Toluene decomposed readily over the entire temperature range in the 750- μ s observation period. Benzyl radical was a major pyrolysis product which rapidly decomposed at the highest temperatures. Other major products were C_2H_2 , C_4H_2 , and CH_4 with lesser amounts of C_2H_4 , C_6H_2 , and C_6H_6 . These observations are in reasonable agreement with earlier reports.^{2–4}

Both gradient and concentration profiles were modeled with various mechanisms based on the example of Table I. As a complete description of this extremely complex pyrolysis, which ultimately generates soot, this mechanism is obviously quite inadequate. It simply represents an attempt to account for dominant reactions among the major species during the early stages of the decomposition. Most reaction rate constants are literature expressions as cited and require no further discussion. However, there are two variant notions which should be explained. In reactions 1–8, two C_7H_7 are identified: C_7H_7 (Bz), the benzyl radical, and C_7H_7 (MP), which stands for all three possible methylphenyl radicals produced by ring abstraction in reaction 3. The evidence for substantial methylphenyl formation is quite convincing even in relatively low temperature toluene pyrolysis.^{19–21} These radicals are here taken to rapidly decompose via (6) and (7), based on a presumed analogy with phenyl dissociation, but may also produce C_3H_3 and C_4H_4 at lower temperatures. This notion can then provide the pressure-dependent path to C_3H_3 , C_4H_4 , C_3H_3 , and C_2H_2 required by the Knudsen cell experiments.^{2,3} At high temperatures, $T > 1500$ K, these reactions of the methylphenyls are of little consequence to either the product distribution or the density gradient. The dissociation of benzyl radical is tentatively envisaged to produce only the products shown in reaction 8, since a direct dissociation to C_4 species, as suggested by Smith,^{2,3} would appear to require an intermediate diradical. With (1a) included, this is no longer needed for C_4 formation.

The results of modeling the LS gradients with various mechanisms having different proportions of reactions 1 and 1a are shown in Figures 1–3. As is evident in Figures 2 and 3, confinement of dissociation to reaction 1 produces a profile which drops much too rapidly at the outset. This is a consequence of the early equilibration of this reaction noted by Colket and Seery.⁶ The small equilibrium constant for this reaction does not permit significant dissociation even at high temperatures. Since the principal secondary reaction



is near thermoneutral, the rapid equilibration of (1) produces a precipitous drop in density gradient (note particularly Figure 3). The experimental profiles show a more gradual reduction of gradient, which is the behavior expected for an effectively irreversible reaction whose rate declines due to reactant depletion and temperature drop only. Such a reaction is nicely provided by (1a). As above, the products (C_6H_5 and C_4H_3) should dissociate with sufficient rapidity⁸ to make the overall reaction effectively



The multiplicity of products then makes this process effectively irreversible.

The one modification of the mechanism which could eliminate the need for (1a) is a large rate of dissociation for benzyl radical, which would then make reaction 1 effectively irreversible. A few modeling studies with dissociation confined to reaction 1 show what is needed is a rate constant for benzyl dissociation faster

TABLE II: RMS Gradient Sensitivities for the Experiment of Figure 2

reaction no. ^b	sensitivity ^a	reaction no. ^b	sensitivity ^a
1	0.067	3	2.1×10^{-3}
1a	0.489	9	0.049
2	0.033	11	0.117 ^c

^aSensitivities are as defined as ref 8, the mean taken over 0.5–3 μ s. Sensitivities for reactions 4–8, 10, and 12–26 are smaller than that of reaction 3. ^bReactions numbered as in Table I. ^cThis sensitivity to (the reverse of) reaction 11 arises from the large amount of propargyl radical (C_3H_3) produced late in the pyrolysis at high temperatures by reaction 8. As such, it is probably an artifact created by our uncertainty regarding both the decomposition of benzyl and the fate of propargyl radical at high temperatures.

than that of (1). Following Figure 4, this would mean a rate constant for reaction 8 greater than 10^4 s^{-1} at 1700 K. For several reasons such a large rate constant is unacceptable. First, this will generate a large positive density gradient immediately following dissociation of ethylbenzene for $T > 1700$ K, where only *negative* gradients are observed (note Figure 3 of ref 12). This observation would suggest 10^4 s^{-1} is almost a factor of 100 too large for reaction 8 at 1700 K. Second, benzyl radical is seen as a major product in the TOF mass spectra reported here for $T > 1700$ K, and this would not be possible with such a rapid dissociation. Finally, although there may be some problems with the interpretation of the UV absorption measurements of Astholtz et al.,¹⁰ they still seem incompatible with a dissociation rate anywhere near this size. The rapid disappearance of benzyl in the highest temperature TOF mass spectra need not imply rapid dissociation of this radical. In the suggested mechanism of Table I, benzyl is quite efficiently removed by recombination to toluene through the reverse of (1) and subsequent dissociation of this via (1a).

The result of attempts to optimize the choice of rate for (1) and (1a) is shown in Figures 1–3. The “optimum” choice of rate constants, whose results are also illustrated, is

$$\log k_{1a} \text{ (s}^{-1}\text{)} = 12.95 - 72.6 \text{ (kcal)} / 2.3RT \quad (1600\text{--}2100 \text{ K, } 0.5 \text{ atm)}$$

and $k_{1a}/k_1 = 2\text{--}3$, for the same conditions. The results are actually quite insensitive to the rate constant for reaction 1, as is evident in the displayed calculations and the sensitivity analysis of Table II; only the rate constant for (1a) is really defined by these experiments. The net endothermic rate of Figure 4 is then almost entirely from (1a). The analysis of Table II also shows that these conclusions are effectively independent of the rest of the mechanism.

The mechanism quite successfully predicts the near-linear behavior of most of the semilog gradient profiles, the slight upward convexity of some low-pressure gradients (cf. Figure 2), and also the strong concavity of the highest temperature profiles as exemplified in Figure 3. Since endothermic dissociation will always have a rate constant decreasing with time as the temperature falls, with no chain acceleration such a process will exhibit concave semilog gradient profiles like that of Figure 3, but will do so under all conditions. As expected, the model calculations show the predominant linearity of these semilog LS profiles results from a slight chain acceleration of the endothermic rate which closely compensates the effect of temperature drop. This acceleration is very weak here, much weaker than it is, for example, in benzene, where it produces a distinct local maximum.⁸ This weakness is another consequence of the stability of benzyl radical. The fast, slightly exothermic, and dominant abstraction of reaction 2 is then not followed by further reaction, neither generating endothermicity nor returning an H atom with which to continue the chain. Toluene remains an effective radical scavenger even at these temperatures. In benzene the opposite is true; abstraction produces unstable phenyl, and this quickly dissociates through strongly endothermic steps which also provide a new H atom.

A further test of the Table I mechanism is provided by modeling of the TOF concentration profiles for major species, as shown in Figures 5–8. The result is really quite satisfactory, the only

(19) Blades, A. T.; Steacie, E. W. R. *Can. J. Chem.* **1954**, *32*, 1142.

(20) Price, S. J. *Can. J. Chem.* **1962**, *40*, 1310.

(21) Takahasi, M. *Bull. Chem. Soc. Jpn.* **1960**, *33*, 801.

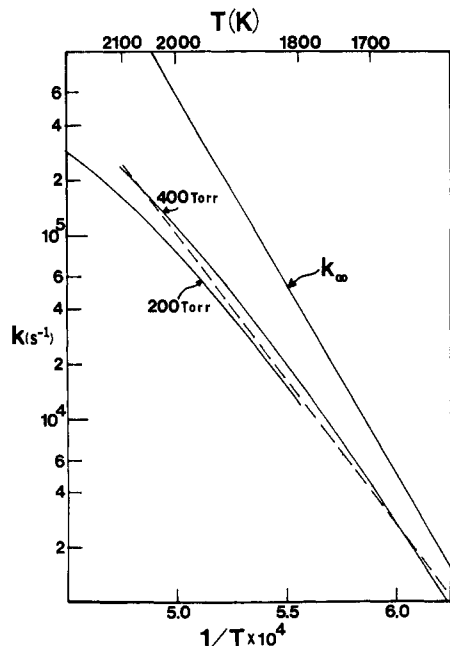
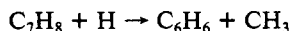


Figure 9. Comparison of a "routine" RRKM calculation (see text) with the expression for k_{1a} at 400 Torr derived here and given in Table I. Here the dashed line shows the derived rate constants for 400 Torr, and the solid lines show the calculated rate constants. The expression for the high-pressure rate is $\log k_{1a}^{\infty} (\text{s}^{-1}) = 16.09 - 94.4 (\text{kcal})/2.3RT$.

discrepancy being the slightly too large C_4H_2 concentrations at high temperatures. We would ascribe this discrepancy to the participation of C_4H_2 in the soot formation process.²² These measurements also offer a strong confirmation of the importance of (1a). Without this channel, for example, using the Szwarc mechanism as given by Rao and Skinner,¹¹ one cannot come within a factor of 2 of the observed CH_4 concentrations. We would emphasize that the rate constant for the substitution



which generates methyl and thus methane in the Szwarc mechanism, was here chosen as the *total* rate constant for addition of H atom to toluene reported by Ravishankara.²³ This should represent an extreme upper limit to the substitution rate at high temperature. If we employ the rate constant actually suggested, and used, by Rao and Skinner¹¹ (footnote b of their Table I), this rate is reduced by a factor of 25–60 over the temperature range applicable here. With such a low rate for this near-thermoneutral reaction, its contribution to the LS profiles would be vanishingly small. It was thus not included in the modeling of these data.

A seemingly unusual aspect of the kinetics is the very low effective activation energy of 72.6 kcal/mol for reaction 1a under present conditions, considering that ΔH°_0 is 102.4 kcal/mol for this reaction. To show that this is actually much as expected, we have run a "routine" RRKM calculation on reaction 1a, ignoring any interference by reaction 1. The calculation uses the usual restricted-rotor Gorin transition state²⁴ with restriction parameter $\eta = 1 - 4.0/T$, which is very near that obtained in a Gorin model fit of ethane dissociation,¹² and a constant $\langle -\Delta E \rangle_{\text{all}} = 100 \text{ cm}^{-1}$. The results are compared to the rate constant expression for (1a) at 0.5 atm given above in Figure 9. The magnitude, slope, and 400–200-Torr falloff (cf. Figure 4) of the calculated rates are all at least roughly correct. At 2000 K, the 400–200-Torr falloff is 30% and the central E_a (for 1850 K, 400 Torr), is 72 kcal/mol. It is evident that all that is needed for agreement with all the LS data to within 10% is a slight reduction in $\langle -\Delta E \rangle_{\text{all}}$. Nonetheless, we have made no attempt to optimize this calculation. For one

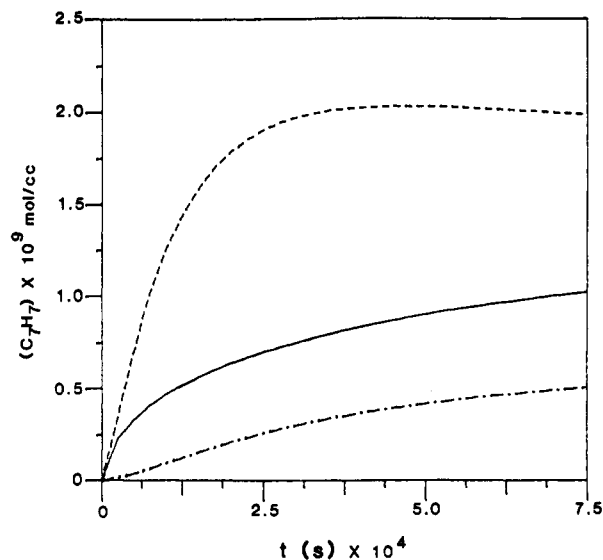


Figure 10. Calculated benzyl radical concentration profiles simulating an experiment of ref 10. Here $T = 1540 \text{ K}$, and initial toluene concentration is $2.2 \times 10^{-9} \text{ mol/cm}^3$. The following lines were calculated by using selected reactions and rate constants from ref 9: (—) reactions 1 and 2 and their reverse only; (---) the same removing the reverse of (1); (-.-) calculated using the complete mechanism shown in Table I.

thing, this is a two-channel dissociation, and these channels will interfere where falloff occurs. Toluene also is so large a molecule that the simple formula relating $\langle -\Delta E \rangle_{\text{all}}$ and β_c used here²⁵ is not valid for much of the present temperature range.²⁶

A comparison with some previous experiments at 1600 K gives the following: present work, $k_{1a} = 1080 \text{ s}^{-1}$; Rao and Skinner,¹¹ $k_1 + k_{1a} = 1040 \text{ s}^{-1} (k_{1D} \times 1.5)$; Colket and Seery,⁶ $k_{1a} \sim 1000 \text{ s}^{-1}$ (extrapolation), in quite close mutual agreement. The large rates for (1) presented by Astholtz et al.⁹ are evidently the result of neglecting secondary reactions in their analysis, in particular the reverse of reaction 1.¹² In Figure 10, we have illustrated the importance of these omissions through model simulations of one of their experiments.¹⁰

Conclusions

The high-temperature pyrolysis of toluene is a complex process which evidently is initiated by two parallel dissociation channels. The present study is able to define the rate of only one of these channels, but it is this, the essentially irreversible CC fission, which governs the reaction progress at high temperatures. These time-resolved measurements of product formation and density gradient thus fully confirm the essential conclusions of Colket and Seery⁶ from their single-pulse shock tube study.

Unfortunately, several important issues in toluene pyrolysis could not be resolved here. One is the question of the actual rate of (1) at high temperature. Although the LS profiles show some sensitivity to this rate, it is slight (Table II), and the uncertainty in the given k_{1a}/k_1 is at least a factor of 2. An independent, but still rough, estimate of the likely partitioning in toluene dissociation can be made by taking a good low-temperature measurement of the rate for (1) and, assuming this is essentially the high-pressure rate k_1^{∞} , comparing this to the k_{1a}^{∞} derived from the present RRKM model. For (1) we extrapolate the expression of Price,²⁰ $\log k_1^{\infty} (\text{s}^{-1}) = 14.8 - 85 (\text{kcal})/2.3RT$, and for (1a), we had $\log k_{1a}^{\infty} (\text{s}^{-1}) = 16.09 - 94.4/2.3RT$. At 1600 K, these rate constants are equal, while at 2000 K, (1a) has twice the rate of (1). These ratios are about half those suggested by the LS data but are

(25) Troe, J. J. *Chem. Phys.* **1977**, *66*, 4745.

(26) Gilbert, R. G.; Luther, K.; Troe, J. *Ber. Bunsenges. Phys. Chem.* **1983**, *87*, 169.

(27) Kiefer, J. H.; Kapsalis, S. A.; Al-Alami, M. Z.; Budach, K. A. *Combust. Flame* **1983**, *51*, 79.

(28) Budach, K. A.; Kiefer, J. H. *Int. J. Chem. Kinet.* **1984**, *16*, 679.

(22) Slysh, R. S.; Kinney, C. R. *J. Phys. Chem.* **1961**, *65*, 1044.

(23) Ravishankara, A. R.; Nicovich, J. A., as quoted in ref 7.

(24) Smith, G. P.; Golden, D. M. *Int. J. Chem. Kinet.* **1978**, *10*, 489. Baldwin, A. C.; Golden, D. M. *J. Phys. Chem.* **1978**, *82*, 644.

probably also acceptable given the low sensitivity of this data to reaction 1.

The rate and especially the products of benzyl radical dissociation are distressingly uncertain. Some benzyl may also be removed through radical attack, with unknown rate and products. The present results show that benzyl is certainly very stable, but

they cannot define its decomposition pathways or their rates.

Acknowledgment. This research was supported by the U.S. Department of Energy under Contracts DE-FG05-85ER/13340 (R.D.K.) and DE-FG02-85ER/13384 (J.H.K.).

Registry No. Toluene, 108-88-3.

Gas-Phase Addition of the Vinyl Cation to Hydrogen and Methane. A Nuclear Decay Study

Simonetta Fornarini[†] and Maurizio Speranza*

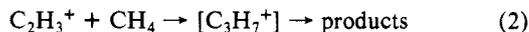
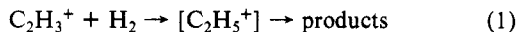
Istituto di Chimica Nucleare del C.N.R., Monterotondo Stazione, 00016 Rome, Italy, and University of Rome, 00100 Rome, Italy (Received: August 12, 1986)

A nuclear technique based on the spontaneous decay of multitruncated precursors that allows the generation of free carbenium ions of exactly the same nature in different environments has been employed for generating the labeled vinyl cation ($C_2X_3^+$, X = H, T) from multitruncated ethylene and for investigating its reactivity toward hydrogen and methane at pressures ranging from 60 to 720 Torr. Kinetic data for the addition of $C_2X_3^+$ to H_2 and CH_4 and the ensuing product distributions are obtained by intercepting the ionic species with different gaseous nucleophiles, i.e., 1,4-dibromobutane, benzene, and methanol, and by isolating the corresponding neutral end products. The results are consistent with the intermediacy of the vinyl cation, formed by the β^- transition with a limited excess of vibrational energy, which inserts into the σ -bonds of H_2 and CH_4 yielding respectively $C_2H_5^+$ and $sC_3H_7^+$ ions. The experiments provide no evidence for the occurrence of alternative $C_3H_7^+$ structures, i.e., protonated cyclopropane, from the $C_2X_3^+$ attack on CH_4 . At CH_4 pressures below 200 Torr, a fraction of the $C_3H_7^+$ adducts fragments directly into allyl cations and H_2 . A definition of the $C_2X_3^+ + H_2$ (or CH_4) addition and fragmentation mechanisms is obtained by comparison of the present data with those arising from previous experimental studies based on different approaches (i.e., radiolysis, ICR, SIFT, HPMS, etc.) and with those of ab initio calculations.

Introduction

A singlet ground-state vinyl cation is the simplest member of the family of unsaturated carbenium ions in which the vacant p orbital of the ^+C center is perpendicular to a strongly polarized π -bond orbital.¹ This electronic configuration confers to the vinyl cation the character of a singlet methylene with a CH_2^+ substituent and, therefore, the ability to insert into σ -type bonds.²

Experimental confirmation of this ability is provided by the significant reactivity of the gaseous vinyl cation toward σ -type molecules. Indeed, addition reactions between the vinyl cation and several simple σ -type molecules, including hydrogen (eq 1) and methane (eq 2), have been actively investigated by a variety



of mass spectrometric approaches, such as the selected ion flow tube (SIFT) technique,³ photoionization,⁴ ion cyclotron resonance (ICR),⁴⁻⁶ and a tandem mass spectrometry.⁷ Special attention has recently been paid to the effect of internal energy upon the reactivity of the vinyl cation toward hydrogen and methane.⁴⁻⁷ As a result of such a sustained effort, a large body of experimental data is currently available concerning rate coefficients and ionic product distribution for these reactions. Unavoidably, the picture obtained by the exclusive application of even powerful mass spectrometric techniques is incomplete, owing especially to the recognized⁸ difficulties encountered by these techniques in the positive structural identification of ionic species. The picture is further blurred by the rapid fragmentation in the low-pressure ion source of the spectrometer of the adduct ions from insertion of $C_2H_3^+$ into H_2 or CH_4 , which prevents their direct isolation and characterization. In this case, isotopic labeling with ^{13}C and

D is the only means to obtain indirect information on the course of the reactions.^{6,7}

A more complete mechanistic view of reactions 1 and 2 is desirable since it provides fundamental information on the carbenoid nature of $C_2H_3^+$, which is of interest, inter alia, to the study of the synthesis of large hydrocarbon molecules in interstellar molecular clouds⁹ and in the atmospheres of the outer planets.^{10,11}

This paper presents the results of a comparative study of the reactivity of $C_2H_3^+$ toward H_2 and CH_4 carried out in the gas phase in the pressure range 60–720 Torr, using ionic reactants from the β^- decay of T atoms in multitruncated ethylene.^{12,13}

The decay technique affords a convenient means to introduce free cations of defined structure and concentration into liquid and gaseous systems and to follow their reactions by radiotracer techniques.¹⁴⁻¹⁷ The wide pressure range accessible to the decay

(1) Stang, P. J.; Rappoport, Z.; Hanack, M.; Subramanian, L. R. In *Vinyl Cations*; Academic: New York, 1979.

(2) Kollmar, H.; Smith, H. O. *Angew. Chem., Int. Ed. Engl.* **1972**, *11*, 635.

(3) Adams, N. G.; Smith, D. *Chem. Phys. Lett.* **1977**, *47*, 383.

(4) Buttrill, S. E., Jr.; Kim, J. K.; Huntress, W. T., Jr.; Le Breton, P.; Williamson, A. *J. Chem. Phys.* **1974**, *61*, 2122.

(5) Kim, J. K.; Anicich, V. G.; Huntress, W. T., Jr. *J. Phys. Chem.* **1977**, *81*, 1798.

(6) Fornarini, S.; Gabrielli, R.; Speranza, M. *Int. J. Mass Spectrom. Ion Processes* **1986**, *72*, 137.

(7) Senzer, S. N.; Lim, K. P.; Lampe, F. W. *J. Phys. Chem.* **1984**, *88*, 5314.

(8) See, for instance, the discussion on the difficulties of the mass spectrometric approach: Cone, C.; Dewar, M. J. S.; Landman, D. *J. Am. Chem. Soc.* **1977**, *99*, 372.

(9) Dalgarno, A.; Black, J. H. *Rep. Progr. Phys.* **1976**, *39*, 579.

(10) Huntress, W. T., Jr. *Adv. At. Mol. Phys.* **1974**, *10*, 295.

(11) Narcisi, R. S. In *Interactions between Ions and Molecules*, Ausloos, P., Ed.; Plenum: New York, 1974.

(12) Fornarini, S.; Speranza, M. *Tetrahedron Lett.* **1984**, *25*, 869.

(13) Fornarini, S.; Speranza, M. *J. Am. Chem. Soc.* **1985**, *107*, 5358.

[†] University of Rome.

* Istituto di Chimica Nucleare del C.N.R., Monterotondo Stazione.